Reflective ghost imaging free from vibrating detectors*

Heng-xing Li(李恒星), Yan-feng Bai(白艳锋)†, Xiao-hui Shi(施晓辉), Su-qin Nan(南苏琴), Li-jie Qu(屈利杰), Qian Shen(沈倩), and Xi-quan Fu(傅喜泉)

College of Computer Science and Electronic Engineering, Hunan University, Changsha 410082, *China*

(Received 5 April 2017; revised manuscript received 24 May 2017; published online 20 August 2017)

The vibration is one of the important factors affecting imaging quality of conventional remote sensing imaging because the relative motion between the imaging system and the target can result in the degradation of imaging quality. The influence of the vibration of the detector in the test path on reflective ghost imaging (RGI) is investigated theoretically and experimentally. We analyze the effects of the vibrating amplitude and velocity. The results demonstrate that the microvibrations of the bucket detector have almost no impact on the imaging resolution and signal-to-noise ratio (SNR) of RGI, i.e., the degradation of imaging quality caused by the vibration of the detector can be overcome to some extent. Our results can be helpful for remote sensing imaging.

Keywords: reflective ghost imaging, vibration, remote sensing

PACS: 42.30.–d, 42.50.Ar, 42.30.Wb, 42.30.Va **DOI:** 10.1088/1674-1056/26/10/104204

1. Introduction

The relative motion between the camera and the object imaged has always been one of the principal factors affecting the quality of conventional imaging. It can result in the degradation of imaging quality, even leading to the difficulty of identifying the imaging content. This unavoidable problem can be solved by shortening the exposure time and adopting the restoration algorithm of post-processing of the image.[1–3] However, these solutions either require very high imaging equipment, or need a long time to deal with. Some algorithms are difficult to achieve in practice. In order to achieve low-cost anti-motion blur imaging, we can consider the use of other imaging methods. As a non-local imaging method in recent decades, ghost imaging has been rapidly developed and widely concerned. According to the theoretical proposal of Klyshko,[4] Shih *et al.* first experimentally realized ghost imaging (GI) and ghost interference.[5] In 2001, Abouraddy *et al.* thought that quantum entanglement was a prerequisite for achieving distributed quantum imaging,[6] which set off an animated discussion. However, Bennink provided an experimental demonstration of ghost imaging by using a classical source in 2002.[7] Since then, the pseudo-thermal source is usually used to achieve ghost imaging.[8–10] The first experimental demonstration of two-photon correlated imaging with true thermal light[11] was reported in 2005. Wang *et al.* showed the macroscopic difference between quantum and classical coincidence imaging[12]. Lenless ghost imaging with thermal light was proposed in 2006.[13] Most lensless ghost imaging is conducted by using the transparent features of the object or with different transmission media.[14–16]

Differing from previous configurations, the first reflected ghost imaging experiment was realized by Meyers *et al.* and their experimental setup captured a ghost-image by counting the reflected photons from the surface of the target object.[17] Computational ghost imaging[18,19] can be realized with a single-pixel detector, which greatly simplified the system of ghost imaging. Erkmen described the applications of computational ghost imaging in remote sensing.[20] Gong and Han proposed a ghost imaging lidar via a sparsity constraints (GISC lidar) system and demonstrated that high-resolution imaging could be realized at a distance about the 1.0-km range[21] and that a three-dimensional (3D) GISC lidar system could be achieved with the GISC method.[22] The range accuracy of 3D ghost imaging ladar[23] and GI with broad distance[24] have been studied. In practice, it is quite common that the imaging target moves while the imaging system keeps relatively static. So the study of the ghost imaging of the moving target is very meaningful. Noted that the ghost imaging with moving target has been investigated in the literature.[25–30]

In some cases, such as air-to-ground detection, the vibration of the detector is inevitable because of the existence of atomospheric turbulence. In this paper, we present the experimental results about the influence of a shaking detector (bucket detector) on the quality of reflective ghost imaging (RGI). The effects of the vibrating velocity and amplitude are investigated. It is found that the resolution of RGI keeps unchanged when the bucket detector shakes slightly, while the corresponding result of direct imaging is affected greatly.

*Project supported by the National Natural Science Foundation of China (Grant Nos. 61372102 and 61571183).

†Corresponding author. E-mail: yfbai@hnu.edu.cn

© 2017 Chinese Physical Society and IOP Publishing Ltd

2. Theory

Figure 1 shows the scheme for reflective ghost imaging with a shaking detector. During this experiment, the pseudo-thermal source (the transverse size $a = 1$ mm) is prepared by illuminating a frequency-doubled pulsed Nd:YAG laser with wavelength $\lambda = 632.8$ nm into a slowly rotating ground glass. Then a nonpolarizing beam splitter divides the source into two beams, which travel along the test and reference arms, respectively. In the test arm, we replace the transmissive double slit mask with the mirror-reflecting double-strip,[31] it is illuminated by the light source at a distance of d_1. A bucket detector (D_t), which is fixed on the moving platform with a precision of 5 microns, is placed at a distance of d_2 from the object and collects the reflected photons. With the help of the motion platform, we can shake the D_t plane with the shaking amplitude A, which is perpendicular to the optical axis. As for the reference arm, a two-dimensional charge-coupled device (CCD) camera D_r is placed at a distance of d_0 from the source.

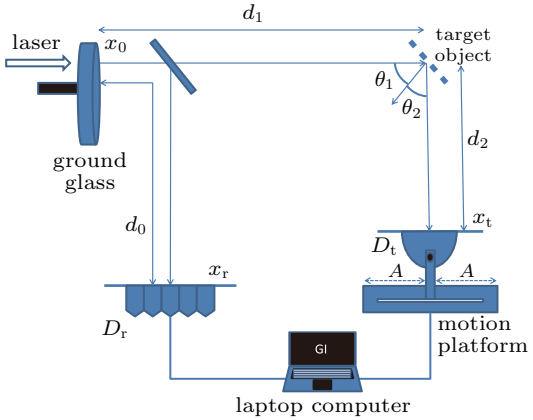


Fig. 1. (color online) Experimental setup for reflective ghost imaging with thermal light.

According to the description of Gatti[32] and Cheng,[33] the second-order correlation function of intensity fluctuations between two detectors is

$$G(x_r,x_t) = \int \mathrm{d}x_1\mathrm{d}x_1'\mathrm{d}x_2\mathrm{d}x_2'\Gamma(x_1,x_1',x_2,x_2') \times h_r(x_1,x_r)h_r^*(x_1',x_r)h_t(x_2,x_t)h_t^*(x_2',x_t), \quad (1)$$

where $\Gamma(x_1,x_1',x_2,x_2') = G^{(1,1)}(x_1,x_2')G^{(1,1)}(x_2,x_1')$, and $G^{(1,1)}$ denotes the first-order correlation function of the light field. x_1, x_2, x_r, and x_t is the coordinate on the source plane, D_t plane and D_r plane, respectively. For a lensless imaging system, under the paraxial approximation, we can get the impulse response $h_r(x_1,x_r)$ in the reference arm,

$$h_r(x_1,x_r) = \frac{1}{\sqrt{\mathrm{j}\lambda d_0}}\exp\left[-\frac{\mathrm{j}\pi}{\lambda d_0}(x_r-x_1)^2\right]. \quad (2)$$

In the test arm, the object consists of two reflected strips instead of a transmittive object. If the surface of the target is sufficiently smooth,[34] the object can be modeled by

$$\langle T^*(x')T(x)\rangle = T^*(x')T(x), \quad (3)$$

where the deterministic pattern $T(x)$ is what we are trying to image. The detector deviation from the optical axis depends on time τ. If the center position of D_t deviates ρ from the optical axis at time τ, x_t can be changed from x_t into $x_t-\rho(\tau)$. According to the Fresnel integral and with the help of Eq. (3), the impulse response $h_t(x,x_t)$ in the test arm can be expressed as

$$h_t(x_2,x_t) = \frac{-1}{\lambda\sqrt{d_1d_2}}\int \mathrm{d}x\exp\left[-\frac{\mathrm{j}\pi}{\lambda d_1}(x_2-x\cos\theta_1)^2\right] \times T(x)\exp\left[-\frac{\mathrm{j}\pi}{\lambda d_2}(x\cos\theta_2-(x_t-\rho(\tau)))^2\right], \quad (4)$$

where θ_1, θ_2 are incident and reflected angles, respectively. Here, we consider $\theta_1 = \theta_2$.

Following along the lines of our other work[35] and substituting Eqs. (2), (3), and (4) into Eq. (1), after simplifying, we can obtain

$$G(x_r,x_t) = \frac{a^2\pi}{\lambda^3 d_0d_1d_2}\int \mathrm{d}x|T(x)|^2 \times \exp\left[-\frac{2a^2\pi^2}{\lambda^2d_1^2}(x\cos\theta_1-x_r)^2\right]. \quad (5)$$

From Eq. (5), the correlation function of intensity fluctuations is independent of the vibration of the test detector for a large enough bucket detector or a small vibrating amplitude. It is noted that equation (5) is the same as Eq. (9) of Ref. [35] in which a static detector is considered. So a small vibrating bucket detector has almost no effect on imaging quality.

3. Experimental results

In our experiment, a reflecting double-strip (two very thin reflected lines, lines width $l = 200$ μm, slit height $h = 1000$ μm, and center-to-center separation equals 800 μm) is chosen as the object imaged.

To highlight the difference between reflective ghost imaging with static and shaking detectors, we first implement static ghost imaging and conventional imaging experiments, and the corresponding results are illustrated in Fig. 2. During this experiment, the relative parameters are chosen as $d_0 = d_1 = 200$ mm, $d_2 = 100$ mm, and $\theta_1 = \theta_2 = \pi/4$. The exposure time of the CCD camera is set to be 1 ms and the sampling frequency is 1.5 HZ. The experimental results depicted in Fig. 2(b) are obtained over 9000 CCD frames. The upper is the imaging pattern, and its cross-section curve is shown in the lower. Similarly, the conventional direct imaging (only the test arm is considered, and the test detector is used as a CCD camera) is shown in Fig. 2(a). To perform a more accurate comparison of image quality, we chose SNR (it was defined as Eq. (6) in Ref. [36]) to compare the quality of RGI with that in conventional imaging. When the detector is static, the SNRs of conventional image and ghost-image are 39.4255 and 2.2620, respectively.

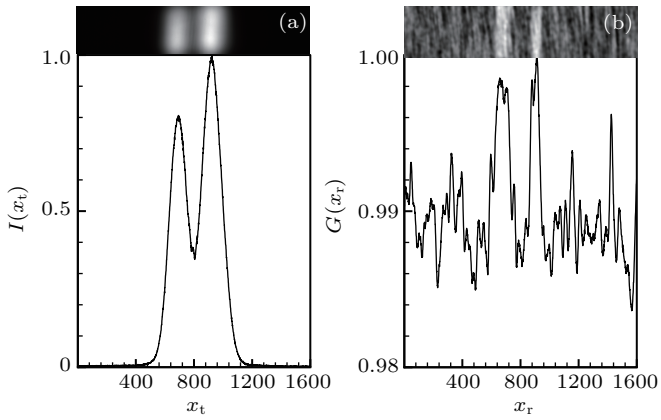


Fig. 2. The acquired image of the double reflective-strip from the two-arm imaging system, (a1) is obtained directly by D_t, panel (b) is obtained in RGI by averaging over 9000 CCD frames.

Then we analyze the effect from the change of the shaking amplitude of the bucket detector on imaging quality. Figure 3 presents the results of conventional imaging and RGI with different shaking amplitudes A. During this process, the shaking velocity of D_t is uniform, here, $V = 19.556$ mm/s. We choose 25 μm as the initial value of A. By comparing Fig. 3(a1) with Fig. 2(a), the resolution of conventional imaging declines when $A = 25$ μm. If we continuously increase the shaking amplitude of the D_t to 150 μm, the moving blurred image is observed, as shown in Fig. 3(a2). When the shaking amplitude is further increased to 500 μm, the imaging pattern appears with some smear tracks, which indicates that the quality of conventional imaging continues to decline. Finally, we increase the shaking amplitude to 900 μm. Obviously, as shown in Fig. 3(a4), the original image cannot be obtained, which means the shaking amplitude is close to the detection limit of the detector. However, it is found that the quality of the ghost imaging has almost no degradation with an increase of A, as plotted in Figs. 3(b1)–3(b3). Note that the ghost imaging of the double strip cannot be observed when $A = 900$ μm, which is beyond the detection range.

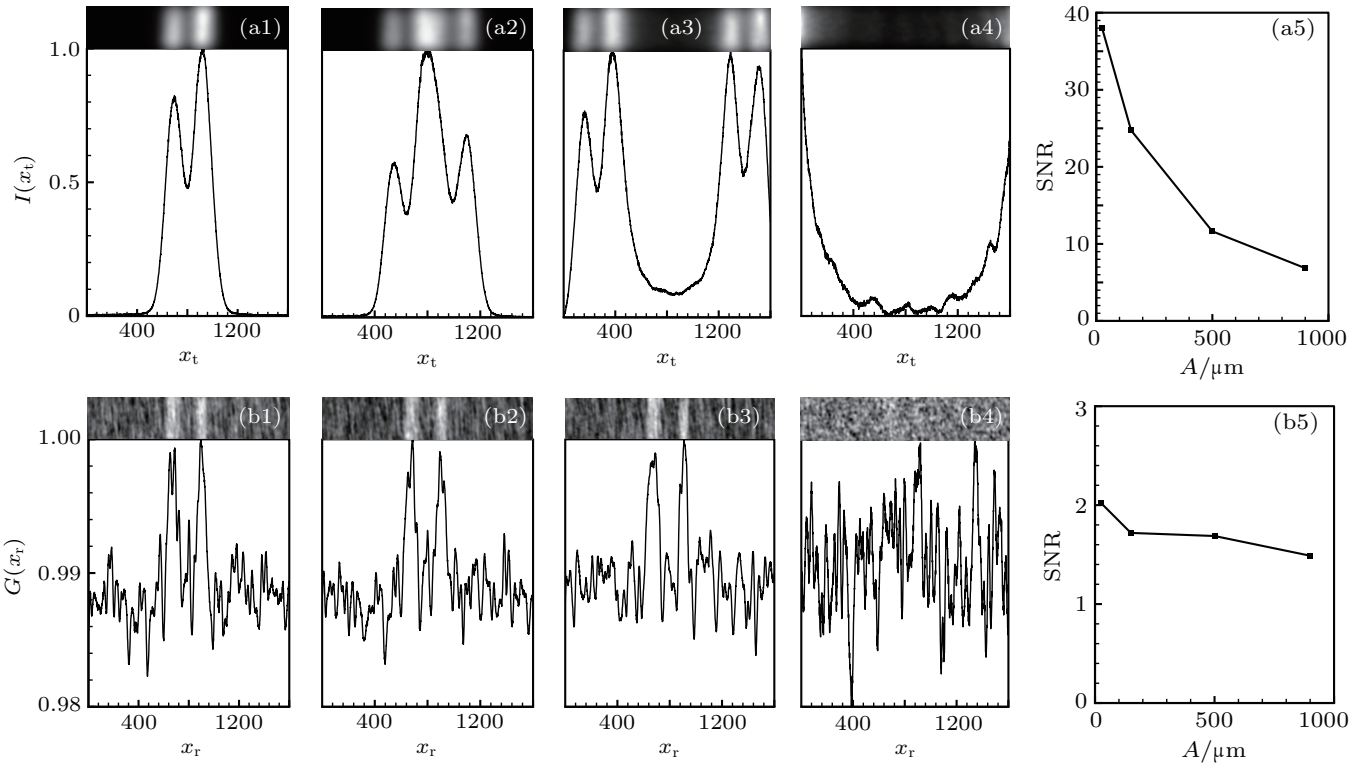


Fig. 3. The reconstructed images of a double reflective-strip under different shaking amplitudes. Panels (a1)–(a4) are the results when only the test arm is considered under $A = 25$, 150, 500, and 900 μm, respectively. Panel (a5) is the corresponding SNR from direct imaging. Panels (b1)–(b4) represents the corresponding results in RGI. (b5) SNR of the ghost-image.

To perform a more accurate comparison, we calculate the signal-to-noise ratio (SNR) which was defined as Eq. (6) in Ref. [36]. The corresponding results are shown in Figs. 3(a5) and 3(b5). It is shown that for both direct imaging and ghost imaging, SNR decreases with an increase of the shaking amplitude of the bucket detector, while the decline is slighter under ghost imaging when compared with that in direct imaging. In other words, the quality of the ghost-image is more stable than that of the conventional imaging with shaking detector.

Next we focus on the effect of the shaking velocity of the bucket detector. Here we keep the experimental parameters ($A = 300$ μm, $d_0 = d_1 = 200$ mm, $d_2 = 100$ mm, $\theta_1 = \theta_2 = \pi/4$) unchanged except for the variety of the shaking velocity V of D_t. The corresponding results are shown in Fig. 4. For small shaking velocity $V = 5.424$ mm/s, the conventional imaging

is poorly performed, as depicted in Fig. 4(a1). The moving blurred image is obtained. When we increase the shaking velocity to 10.771 mm/s, and 19.556 mm/s, the quality of the conventional imaging is still very poor. However, for the corresponding ghost imaging shown in Figs. 4(b1)–(b3), the ghost-image with good quality can always be obtained. It is also noted that SNR decreases slightly when the vibrating speed is increased for the two imaging systems, as shown in Fig. 4(b4). From the results, the quality and SNR of RGI are insensitive to V.

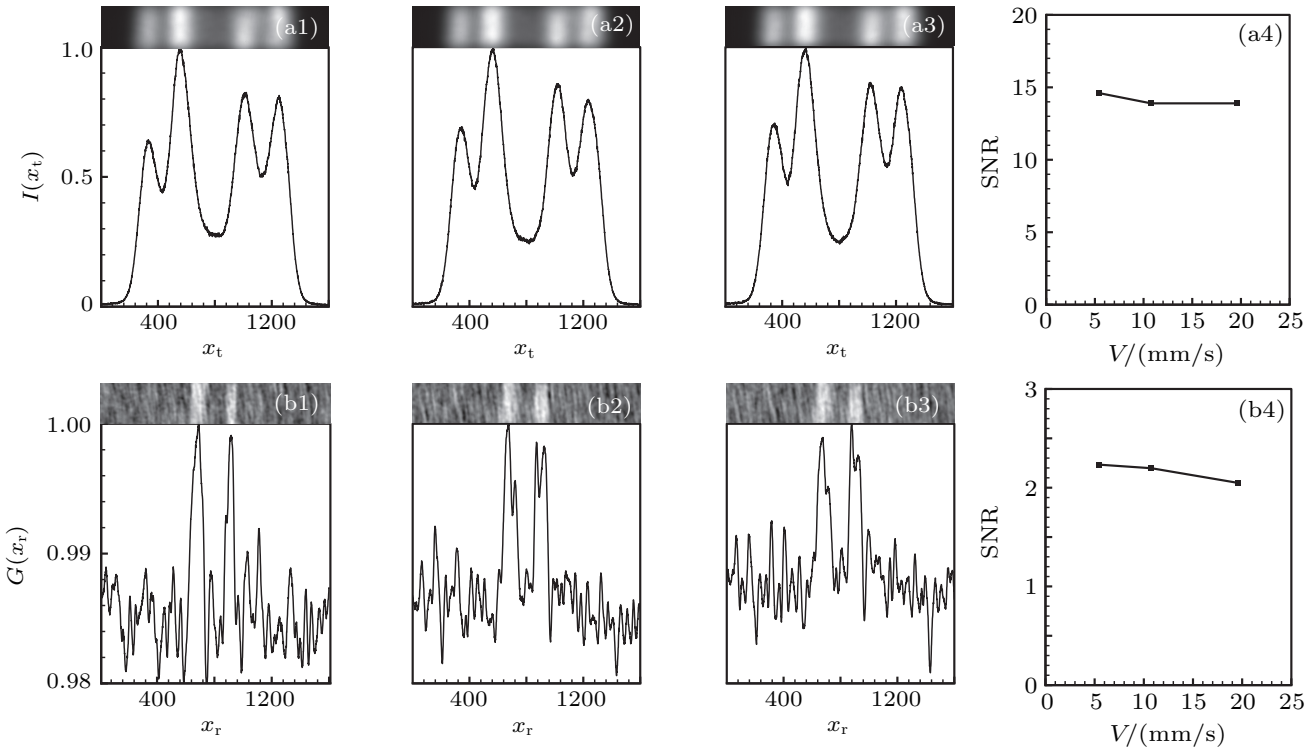


Fig. 4. (a1)–(a3) The results from conventional imaging when $V = 5.424$ mm/s, $V = 10.771$ mm/s, $V = 19.556$ mm/s, respectively. (a4) Relationship between the SNRs of conventional imaging and V. (b1)–(b3) The corresponding results in RGI. (b4) The dependence of SNRs of RGI on V.

4. Conclusion

In conclusion, we have investigated the influence of the detector's vibration on the imaging quality of the reflective ghost imaging. Under different vibrating amplitudes and velocities of the test detector, the performance of the conventional imaging and the ghost imaging are quite different. The quality of the conventional imaging becomes worse with the increase of the shaking amplitude and velocity. However, the constructed ghost-image in RGI has almost no changes. That is to say, RGI can overcome the motion blur caused by the relative micro-motion between the test detector and the target, and gain a ghost-image with better quality.

References

[1] Rav-Acha A and Peleg S 2005 *Pattern. Recogn. Lett.* **26** 311

[2] Lokhande R, Arya K and Gupta P 2006 *Proceedings of the* 2006 *ACM symposium on Applied computing*, April 23–27, 2006, Dijon, France, p. 301

[3] Shan Q, Jia J and Agarwala A 2008 *ACM SIGGRAPH* 2008 *papers*, August 11–15, 2008, Los Angeles, California, p. 73

[4] Klyshko D 1988 *Sov. Phys. Usp.* **31** 74

[5] Pittman T, Shih Y, Strekalov D and Sergienko A 1995 *Phys. Rev. A* **52** R3429

[6] Abouraddy A F, Saleh B E, Sergienko A V and Teich M C 2001 *Phys. Rev. Lett.* **87** 123602

[7] Bennink R S, Bentley S J and Boyd R W 2002 *Phys. Rev. Lett.* **89** 113601

[8] Ferri F, Magatti D, Gatti A, Bache M, Brambilla E and Lugiato L A 2005 *Phys. Rev. Lett.* **94** 183602

[9] Wang K G and Cao D Z 2004 *Phys. Rev. A* **70** 041801

[10] Cao D Z, Xu B L, Zhang S H and Wang K G 2015 *Chin. Phys. Lett.* **32** 114208

[11] Zhang D, Zhai Y H, Wu L A and Chen X H 2005 *Opt. Lett.* **30** 2354

[12] Cao D Z, Xiong J and Wang K G 2005 *Phys. Rev. A* **71** 013801

[13] Scarcelli G, Berardi V and Shih Y H 2006 *Appl. Phys. Lett.* **88** 061106

[14] Cheng J 2009 *Opt. Express* **17** 7916

[15] Gong W L and Han S S 2011 *Opt. Express* **36** 394

[16] Turiaci G J, Varga J J M and Iemmi C 2013 *Optik - International Journal for Light and Electron Optics* **124** 6212

[17] Meyers R E, Deacon K S and Shih Y H 2007 *J. Mod. Opt.* **54** 2381

[18] Shapiro J H 2008 *Phys. Rev. A* **78** 061802

[19] Phillips D B, He R, Chen Q, Gibson G M and Padgett M J 2016 *Opt. Express* **24** 14172

[20] Erkmen B I 2012 *J. Opt. Soc. Am. A* **29** 782

[21] Zhao C Q, Gong W L, Chen M L, Li E R, Wang H, Xu W D and Han S S 2012 *Appl. Phys. Lett.* **101** 141123

[22] Gong W L, Zhao C Q, Yu H, Chen M L, Xu W D and Han S S 2016 *Sci. Rep.* **6** 26133

[23] Yang X, Zhang Y, Xu L, Yang C H, Wang Q, Liu Y H and Zhao Y 2015 *Chin. Phys. B* **24** 124202

[24] Duan D Y, Zhang L, Du S J and Xia Y J 2015 *Chin. Phys. B* **24** 104203

[25] Li H, Xiong J and Zeng G H 2011 *Opt. Eng.* **50** 127005
[26] Li E R, Bo Z W, Chen M L, Gong W L and Han S S 2014 *Appl. Phys. Lett.* **104** 251120
[27] Zhang C, Gong W L and Han S S 2013 *Appl. Phys. Lett.* **102** 021111
[28] Li X H, Deng C J, Chen M L, Gong W L and Han S S 2015 *Photon. Res.* **3** 153
[29] Gao Y, Bai Y F and Fu X Q 2016 *Opt. Express* **24** 25856
[30] Zeng X, Bai Y F, Shi X H, Gao Y and Fu X Q 2017 *Opt. Commun.* **382** 415
[31] Basano L and Ottonello P 2010 *Opt. Commun.* **283** 2657
[32] Gatti A, Brambilla E, Bache M and Lugiato L A 2004 *Phys. Rev. Lett.* **93** 093602
[33] Cheng J and Han S S 2004 *Phys. Rev. Lett.* **92** 093903
[34] Gong W L 2016 *J. Optics-UK* **18** 085702
[35] Nan S Q, Bai Y F, Shi X H, Shen Q, Li H X, Qu L J and Fu X Q 2016 *IEEE P. J.* **9** 7500107
[36] Song S C, Sun M J and Wu L A 2016 *Opt. Commun.* **366** 8